small NANO MICRO

Nanolocomotion — Catalytic Nanomotors and Nanorotors

Tihana Mirkovic, Nicole S. Zacharia, Gregory D. Scholes, and Geoffrey A. Ozin**

Nature's nanomachines, built of dynamically integrated biochemical components, powered by energy-rich biochemical processes, and designed to perform a useful task, have evolved over millions of years. They provide the foundation of all living systems on our planet today. Yet synthetic nanomotors, driven by simple chemical reactions and which could function as building blocks for synthetic nanomachines that can perform useful tasks, have been discovered only in the last few years. Why did it take so long to power-up a myriad of synthetic nanostructures from their well-known static states to new and exciting dynamic ones of the kind that abound in nature? This article will delve into this disconnect between the world of biological and abiological nanomotors, then take a look at some recent developments involving chemically powered nanoscale motors and rotors, and finally try to imagine: what's next for nanolocomotion?

Keywords:
- catalytic propulsion
- nanolocomotion
- nanomotors
- nanorotors

1. Introduction

1.1. Motivation

One of the aspiring goals of nanotechnology is the fabrication of miniaturized machines, which could either be analogous to existing macroscopic versions, or they could be based on entirely new principles. A machine, considered to be a device constructed to perform a useful task whereby it uses power, has not only been the product of human design. Indeed, nature has over billions of years perfected in an enormous variety and sophistication a nanoscale world fuelled with chemical and light energy in which factories of self-replicating and self-repairing nanomachines operate under superb control and execute translational and rotational movement with high precision.

The field of synthetic nanomachines spans from a molecular scale to micrometer dimensions. The advances in molecular machine design, which incorporates the utilization of either light or chemical energy, has recently been reviewed elsewhere.[1] A number of excellent reports[2–4] have been published recently summarizing advances and discussing the challenges that the field of artificial nanomotors, which are exhibiting near-micrometer dimensions, is facing. Here, we try to give an alternative perspective by making direct comparisons and drawing parallels between the motility exhibited by a synthetic system composed of catalytic nanorod motors and a biological organism, a flagellar alga, whose propulsion mechanism was derived through natural evolution.

[*] Prof. G. A. Ozin, Dr. T. Mirkovic, Prof. G. D. Scholes
Department of Chemistry, University of Toronto
80 St. George Street, Toronto, M5S 3H6 (Canada)
E-mail: gozin@chem.utoronto.ca
Prof. N. S. Zacharia
Department of Mechanical Engineering, Materials Division
Texas A&M University, 3123 TAMU, College Station, TX 77840 (USA)
E-mail: nzacharia@tamu.edu

Supporting Information is available on the WWW under http://www.small-journal.com or from the author.

DOI: 10.1002/smll.200901340

1.2. Biological Nanomotors

Nature's nanoscale devices can be broadly divided into three categories: DNA-based, protein-based, and chemical molecular motors. One of the typical examples of a biological factory is the organelle ribosome, which consists of ribosomal RNA (rRNA) and protein. Together they are able to read messenger RNAs and translate the encoded information into proteins. More recently, the construction of a DNA machine, which resembles a pair of tweezers, has been reported,[5] where the DNA is used not only as a structural material, but also as ''fuel.'' The construction and operation of the molecular tweezers, composed of three strands of DNA, are illustrated in Figure 1a.

Some of the notable forms of motor proteins include kinesins, myosins, and dyneins, which are used in diverse processes from muscle contraction to vesicle movement. These motors harness the chemical free-energy released by the hydrolysis of adenosine 5′-triphosphate (ATP) and perform

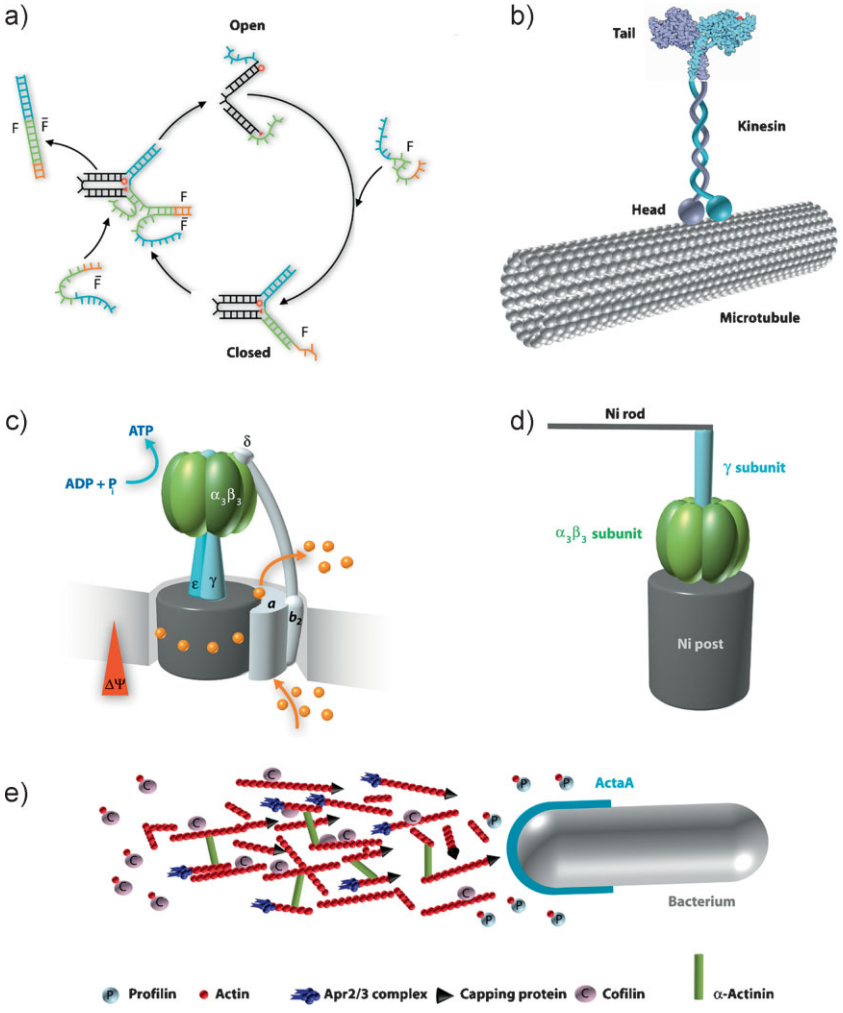

Figure 1. Examples of biological and hybrid nanomotors. a) Construction and operation of the molecular tweezers. It may be closed and opened by addition of auxiliary strands of "fuel" DNA, where each cycle produces a duplex DNA waste product. b) The twin heads of kinesin alternately bind the microtubule as the protein moves. c) Schematic representation of ATPase and its hybrid analogue (d). e) Molecular components required for actin-based motility of *Listeria monocytogenes*. The *Listeria* continues to move as the polymerization progresses, generating a "comet tail" of actin filaments in the direction opposite of its motion.

different mechanical functions while translating with a "hand-over-hand" mechanism along cytoskeletal filaments (Figure 1b).[6]

Some molecular machines seem similar to the more familiar human-scale analogues, such as the F_0F_1-ATP synthase, a membrane protein complex that uses electro-osmotic energy from a transmembrane proton or sodium ion gradient to synthesize ATP from adenosine 5′-diphosphate (ADP) and inorganic phosphate, and whose rotary motor design superficially resembles an electric motor (Figure 1c).[7] The proton-gradient-driven motors, displaying higher complexity than the one discussed above, have also been observed to be the driving force behind flagellar filaments, which are used by many micro-/nanoscale swimmers as propellers.[8]

Another well-studied biological nanomachine is the bacterium *Listeria monocytogenes*, whose motility is attributed to an asymmetrical design that allows for the non-uniform expenditure of locally available energy (Figure 1e). The pathogen has non-uniformly distributed ActA proteins on its surface, which are able to catalyze the production of actin filaments from the actin monomers in the cytoplasm of the host cell. The asymmetry in the ActA location on the cell surface leads to the asymmetric production of actin filament clouds, which, once dense enough, contribute to the recoil motion of the *Listeria* from the relatively immobile network of actin filaments.[9,10]

1.3. Hybrid Nanomotors

A new class of nanomotors is hybrid nanomachines based on the integration of biomolecules with nano- or microinorganic components. Theriot et al. have demonstrated that, through the asymmetrical surface functionalization of nonbiological objects with the catalytic ActA, they can be rendered mobile in an actin-rich environment.[11] Montemagno et al.[12] demonstrated another hybrid system, an organic–inorganic propeller, in which the rotary ATPase enzyme was exploited to drive the submicrometer-sized nickel rods in the presence of ATP fuel as depicted in Figure 1d.[12] Exploiting the mobility of microorganisms to perform useful tasks, such as moving microscale loads, has been explored by Whitesides et al., where polystyrene beads were attached to photosynthetic unicellular algae.[13]

2. Learning from Nature

Problems encountered in hybrid systems usually stem from trying to adapt biological motors outside their natural environment. Sometimes it is not trivial, while other times it might not be useful for a certain application, to replicate in vivo conditions. Even though biology provides an extraordinarily developed repertoire of bio-nanomachines, their full replication due to their substantial structural complexity is not achievable with today's technology. We should be able to extract key concepts and principle functionalities of biomotors to help us devise variants that we could adapt to display useful functionalities. In addition to starting from simple biomimetic systems, we need to research the basic principles behind the functional mechanisms of dynamic nano-objects in the hope that they will become a basis for artificial nanomachine design and nanotechnology.

2.1. Bar-Coded Nanorods

Recently motors and rotors made of bimetal nanorods have been discovered in which propulsion is induced by a chemical reaction occurring on a catalytic segment of the nanorod.[14,15] By understanding the origin of the motion of these nanorods it should be possible to devise ways to control their motion and

small NANO MICRO

use this knowledge to design and build nanomachines that perform a useful task. The basic units of these systems are metal nanorods: cylindrical constructs with a diameter in the range of 10–500 nm and length from one to several micrometers. A versatile synthetic method for accessing these structures is the electrochemical deposition of metals within the cylindrical channels of a nanoporous membrane.[16] The longitudinal modulation in composition also provides numerous opportunities for assembling functional nanorod architectures. For instance, ferromagnetic segments enable bar-coded metal nanorods to be magnetically organized into end-connected chains[17] and side-assembled bundles.[18]

In the context of nanolocomotion, chemically powered linear motion of an Au–Pt nanorod has been observed in an aqueous H_2O_2 environment,[14,19] while rotational motion of Au–Ni nanorods results when one end is tethered to a silicon surface.[15] These recent developments in chemical nanolocomotion have raised the intriguing possibility of assembling nanomachines with metal nanorods.[4,20] In systems such as these self-propelled nanorods, each object is able to generate its own field or motive force, thus achieving independent autonomous motion. In multisegmented nanorods, the catalytic metal segment (Pt or Ni) is employed in the decomposition of H_2O_2, which can be used to translate the free chemical energy of the surroundings into asymmetric gradients, which result in direct mechanical motion.

These nanolocomotors could be envisioned as nanoscale analogues of human-scale submarines, but the laws governing nano-/microscale robots are quite different from the Newtonian mechanics domain that applies to macroscale robots. Nano-objects find themselves in a very different environment in which all flow is laminar and viscous forces are paramount. In what follows we first explore the dynamical behavior of nanorods in pure water, gaining an insight into Brownian mobility of nanorods. This motion will then be compared with chemically powered motion of the same nanorods induced by H_2O_2 fuel.

3. Brownian Diffusion

Brownian diffusion is described as irregular motion consisting of straight-line movements and rotations where motion is independent of the chemical makeup and physical density of the particle. Einstein gave the theoretical analysis for this observation, where particles in an ensemble move independently of one another, relating the molecular motion to the macroscopic measurement of diffusion characterized by the diffusion coefficient D.[21] Mathematically, the diffusion of a particle in one dimension over time, t, is given by

$$\langle x^2 \rangle = 2Dt \tag{1}$$

The relation can be further generalized for motion in two dimensions (e.g., a membrane) as $\langle r^2 \rangle = \langle x^2 \rangle + \langle y^2 \rangle = 4Dt$ or three dimensions (e.g., a solution) as $\langle r^2 \rangle = \langle x^2 \rangle + \langle y^2 \rangle + \langle z^2 \rangle = 6Dt$, since one can assume that the motions in the x, y, and z directions are statistically independent.

Einstein and Smoluchowski showed that the diffusion of a particle (D) moving through a specific medium is related to the friction coefficient (f) according to

$$D = \frac{kT}{f} \tag{2}$$

where k is the Boltzmann constant and T represents temperature. Stokes highlighted that f depends on the shape of the body, where for a sphere of radius r, $f_{\text{sphere}} = 6\pi\eta r$ (Stokes's law), where η is the fluid viscosity. The combination of Stokes's law and Equation (2) gives the well-known Stokes–Einstein equation

$$D = \frac{kT}{f} = \frac{kT}{6\pi\eta r} \tag{3}$$

In more complex systems, such as where asymmetries in viscous drag play a big role, one has to consider the shape and the orientation of the diffusing particle. Expressions for the frictional drag coefficients of particles of different geometries, such as disks and ellipsoids, and formulas taking into consideration the continuous changes in particle orientation make it possible to estimate the hydrodynamic properties of objects of complex shape.[22]

The dynamical properties of spherical objects have been studied in great depth, but their anisotropic counterparts have not received the same attention despite the existence of a huge variation of nanoscale objects with high aspect ratios including nanowires, nanorods, and nanotubes, but also organisms such as bacteriophage viruses. These kinds of nano-objects could be used as primary building blocks for making self-assembled nanoelectronic, nano-optical, nanomechanical, and nanofluidic circuits and nanoscale machines, and as such understanding the dynamical properties of the suspensions of these anisotropic particles in solution as well as in contact with surfaces is crucial for the realization of functional self-assemblies.

3.1. Diffusion Coefficient of Bar-Coded Metal Nanorods

The estimation of the diffusion coefficient can be either obtained through ensemble or trajectory diffusion.[23] Spectroscopic and electrochemical techniques allow for the determination of the diffusion coefficient through the measurement of ensemble diffusion, and are usually employed in systems where individual particles are not observable. For larger particles, trajectory diffusion is directly observed by microscopy. Both experimental approaches, based on ensemble and trajectory diffusion, should yield diffusion coefficients of the same value.

In our work, we employed trajectory-diffusion experiments to study the dynamics of metal-nanorod suspensions near the surface of the substrate. Quick sedimentation of metal nanorods is expected, as it tends to prevail over diffusion for heavy metal particles of this size (specific gravity = 19.3 for Au), confining the diffusion mobility to two dimensions. St. Angelo et al.[24] investigated the diffusion of gold nanorods on chemically functionalized surfaces and discovered that there is a dominating particle–substrate interaction, which leads to lower than expected observed diffusion coefficients. We investigated the effect of solvent viscosity on the diffusion of

metal nanorods in the vicinity of the glass substrate by measuring the diffusion coefficient of particles suspended in water ($\eta_{water} = 1.005$ cP at 20 °C) and in 40% glycerol ($\eta \approx 4.5 \times \eta_{water}$). The details of the experiment can be found in the Supporting Information and the results are summarized in Figure S1. The measured diffusion coefficient of the nanorods in water was 0.1 $\mu m^2\ s^{-1}$ and that in 40% glycerol was evaluated to be 0.067 $\mu m^2\ s^{-1}$. The theoretical diffusion coefficient is evaluated using a variation of Equation (3), which takes into account the anisotropic geometry of nanorods

$$D = \frac{kT}{f} = \frac{kT}{\frac{4\pi\eta a}{\ln\frac{a}{b} - \frac{1}{2}}} = 0.34\ \mu m^2 s^{-1} \quad (4)$$

where a is the semi-major axis, and b is the semi-minor axis of an ellipsoid, which is moving lengthwise. The theoretical diffusion coefficient is higher than the experimentally observed values. Additionally, the diffusion coefficients of nanorods in water and in 40% glycerol do not differ as much as one would have expected based on the variation in viscosity of the two mediums. These observations are suggestive of a model where hydrodynamic coupling of the particle to the surface of the substrate[25] is occurring and the particles are diffusing through a two dimensional fluid and experience some mobility retardation due to frictional surface interactions, which might dominate the diffusional behavior of these nanorods, causing deviations from simple Stokes–Einstein behavior.

4. Self-Propelled Nano-/Microscale Objects

Despite the high occurrences of Brownian diffusion in natural systems, self-propulsion is required for improving the efficiency of transportation at the nanoscale. Successful fabrication of self-propelled nano-objects will require us to realize that the macroscopic world that we live in and where we have developed our intuitions is very different from the one inhabited by the majority of creatures that surround us, whose dimensions are at the cellular length scale. The usual swimming mechanism for a person in water is based on a periodical motion and inertial effects.[26,27] On the other hand, the self-propulsion of microscopic objects, one of the most remarkable of which are flagellated bacteria, is dominated by viscous forces, whereas inertial movements are nonexistent. This hydrodynamic regime is characterized by a very low Reynolds number, a dimensionless parameter that refers to the relative scales of the object, its inertial forces, and the viscous forces. The Reynolds number is

$$R = \frac{vL\rho}{\eta} \quad (5)$$

where v is the velocity, L refers to the particle dimension, and ρ is the specific gravity of the fluid. Even though we live in the macroscopic world, our cells function in the low Reynolds number regime. The important implication here is that on the cellular scale there is an absence of momentum, and thus cells function without momentum. In the fields occupied with the miniaturization of macro-world machines that rely on momentum, one has to keep in mind that the dynamics of nanomachines could be drastically different, and thus their use in cells could be limited if no adaptations are considered.

5. Mobility Modes of Chemically Powered Metal Nanorods in H_2O_2 Fuel

As mentioned earlier, bar-coded metal nanorods with inbuilt catalytic asymmetry have recently been discovered as a new class of nanomotors. The electrochemically fabricated particles, composed of Au–Pt[14] or Au–Ni[15] segments have been shown to be capable of catalyzing the decomposition of H_2O_2 according to

$$2H_2O_2 \rightarrow 2H_2O + O_2$$

When placed in an aqueous solution of the peroxide fuel the catalytic transformation to water and oxygen at the surface of the bimetallic nanorod presents the key driving force behind the chemically induced locomotion of these nanomotors. But how does this work?

A number of different mobility modes have been observed for these catalytically driven nanomotors. Initially, chemically powered linear motion was reported for Au–Pt[14] and rotational motion for Au–Ni nanorods, where in the latter case one end of the nanorod was tethered to the surface of the substrate.[15] In continuing to work on this system we have discovered that there is even a larger variety of locomotion types that these particles undergo. Figure 2 summarizes the motility behaviors of bimetallic Au–Pt nanomotors with additional information available in Figures S2 and S3. It is usually observed that in a given sample most nanorods move straight in their axial direction with occasional turns (Figure 2a). A smaller proportion of the particles undergo rotational motion, for which three different kinds have been

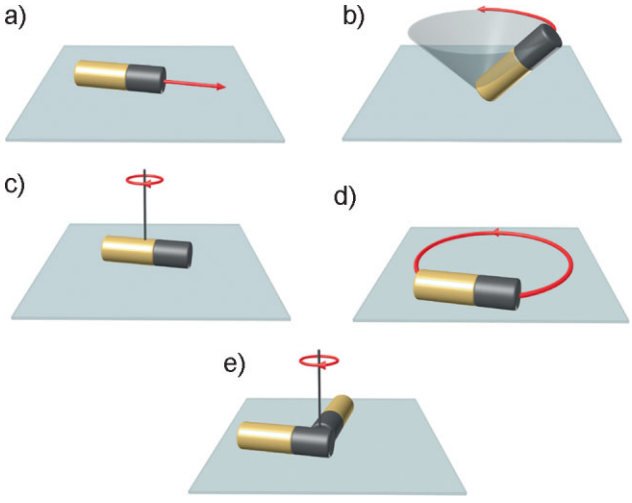

Figure 2. Types of motion observed for bimetallic Au–Pt nanorods in H_2O_2. a) The most commonly observed motion is straight with turns occurring stochastically. Nanorods can also rotate with either one end tethered to the substrate with a varying angle with the plane (b) or spin around its center of mass (c). Some nanorods move around an orbit with varying radii (d). Most cooperative mobility with two or multiple nanorods tends to be rotational (e).

small NANO MICRO

noted. The first resembles the movement of the arm of a clock, where one of their ends is tethered to the substrate (Figure 2b), whereas the second is based on nanorods that circulate around their center without being fixed on the substrate (Figure 2c). Some nanorods also trace out circular orbits (Figure 2d). In additional to the observed motion of individual rods, aggregates of two or more nanorods have also been observed to assemble and undergo mostly rotational motion. Figure 2e illustrates a case of cooperative motion of a two-nanorod aggregate, whereas negative, non-synchronized interactions have also been noted.

6. Nanorod Mobility: Quantified

To quantify and gain a better understanding of the motility of these bimetallic nanomotors, a number of different nanorods were followed over the course of 100 frames (10 frames s^{-1}) in the presence of H_2O_2. The different particles that were tracked are illustrated in Figure 3a together with their corresponding traces, showing the nanorods at their $t=0$ position. As seen from their trajectories, all particles except for nanorod 2 undergo straight propulsion with some turns, whereas nanorod 2 exhibits rotational motion. Over the course of 10 s, the accumulated distance for each nanorod was recorded (Figure 3b) as well as the instantaneous velocity of each particle (Figure 3c), with rod 1 reaching a velocity as high as 40 $\mu m\ s^{-1}$. Visualization and quantification of the rotational motion of these catalytically powered nanomotors is illustrated in Figure 3e and f, where a non-rotating nanorod is contrasted to a rotating one with a period of rotation of ≈5 s. The diffusion coefficients of the presented nanomotors were evaluated at $D_1 = 14.5\ \mu m^2 s^{-1}$, $D_3 = 9.97\ \mu m^2\ s^{-1}$, $D_4 = 5.31\ \mu m^2\ s^{-1}$, and $D_5 = 2.41\ \mu m^2\ s^{-1}$.

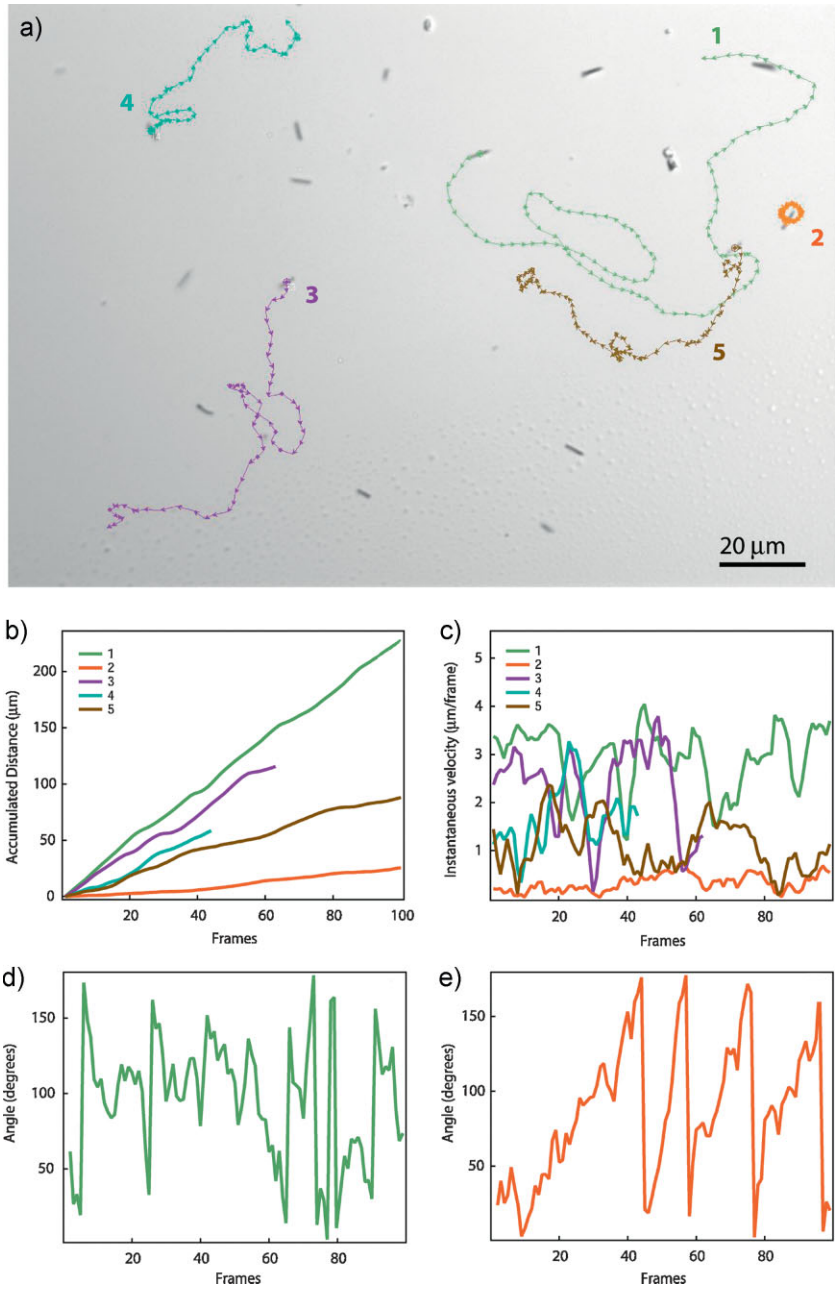

Figure 3. Dynamics of Au–Pt nanorods in the presence of H_2O_2. a) Traces of five different nanorods over the course of 100 frames (10 s). b) Accumulated distance and c) instantaneous velocity of each analyzed nanorod over the course of 100 frames (10 s). d,e) Analysis of directional change of Au–Pt nanorods in the presence of H_2O_2. d) Nanorod 1 from (a) shows random changes in direction as the angle between its long axis and the normal fluctuates without a particular pattern. e) Nanorod 2 from (a) is rotating as is evident from the fluctuation of the angle between its long axis and the normal between 0° and 180°.

The conventional diffusion coefficient is not the ideal measure of the mobility of self-propelled objects, as it does not display the same degree of randomness as particles undergoing Brownian motion. Typical, non-rotating nanorods, just like swimming bacteria, alternate between relatively straight motion, runs, and the shorter, more erratic tumbles. The increased directionality of self-propelled objects originates from the longer lasting runs, whereas tumbles are responsible for the occasional large changes in direction. Lovely and Dahlquist[28] derived an expression for the diffusion of swimming bacteria, which is also applicable to nanorods displaying the mode of motion illustrated in Figure 3a, where the organism is assumed to move at constant speed v along a trajectory composed of a sequence of exponentially distributed straight runs of mean duration τ

$$D = \frac{v^2 \tau}{3(1-\alpha)} \quad (6)$$

where α is the mean value of the cosine of the angle between successive runs.

It is evident that upon progressing from Brownian diffusion to self-propulsion through the addition of H_2O_2 the catalytic activity of metal nanorods resulted in a marked increase of diffusibility of these nano-objects. A number of strategies have recently been employed to further increase observed velocities, such as the incorporation of carbon nanotubes (CNTs) into the Pt component of asymmetric metal nanorods. Increased catalytic activity resulted in average speeds reaching up to 60 $\mu m\ s^{-1}$ in an aqueous solution of H_2O_2 and observing a further acceleration through the addition of hydrazine of up to 200 $\mu m\ s^{-1}$.[29] Dramatic acceleration of bisegment nanorod motors to over 150 $\mu m\ s^{-1}$ has also been achieved using an Ag/Au alloy instead of a Au segment.[30] Similarly, increased surface roughness and the introduction of porosity into the catalytic segment resulted in an increased surface area, leading to an enhancement of the catalytic breakdown of H_2O_2 and ultimately causing the acceleration of metallic nanorods that scaled with surface area.[31]

7. Chemically Induced Locomotion Mechanisms

Over the past few years a number of different systems have been developed that utilize the catalytic activity of a metal surface to power objects of various dimensions ranging from centimeters to nanometers. The chemical reaction that is responsible for the propulsion of these objects is the surface-catalyzed decomposition of H_2O_2 to H_2O and O_2. While superficially simple, the details of how H_2O_2 transforms to H_2O and O_2 at the water–nanorod interface are not understood, and neither are the potential interactions of the self-propelled objects with the substrate surface.

The first artificial motor based on a catalytic reaction was a 1-cm poly(dimethyl siloxane) (PDMS) plate with a small area of Pt defined on one surface of the structure.[32] Analogous to the macro-world, it was observed that these floating plates located at the air–water interface moved autonomously as a result of the thrust created by ejecting small bubbles of gas that formed by the catalytic decomposition of the liquid H_2O_2 fuel. More recently, microtubular microjets that are self-propelled by the recoiling of highly accumulated oxygen microbubbles have also been realized.[33] Similarly, the system designed by Feringa et al.[34] comprising three key elements — a silica microsphere to be transported, a chemical spacer/tether, and a catalyst, a manganese-based catalase mimic — was observed to undergo translational motion as a result of the expansion of oxygen bubbles whose nucleation sites were inhomogeneously distributed on the surface of the particle.

The lithographically fabricated nanorotors by Catchmark et al.[35] were also based on the presence of Pt to impart catalytic asymmetry to the structure. What was interesting about the rotary motion of this nanorotor was that the object moved towards the region of high concentration of oxygen, rather than away, which would have been expected in a bubble-jet-propulsion mechanism observed in these larger structures described above. That peculiar directionality of motion, towards the catalytic end and the higher concentration of the oxygen product, is also shared by our catalytic bar-coded nanorods. Observing in situ nucleation and growth and location of nanobubbles on the nanorods and unambiguously defining their role, if any, in the movement of the nanorods turns out to be a challenge. The mechanism of bubble propulsion can therefore not be used as the only physical concept that drives the observed autonomous motion of nanorods.

The first theory that tried to describe the motion of catalytic rods was based on the oxygen concentration gradient originating from the catalytically active Pt surface. Calculations shortly after showed that this kind of diffusiophoretic contribution alone would not result in a large enough driving force to explain the observed motion. The diffusiophoretic mechanism also predicted motion in the wrong direction.[20] Mallouk et al. still took the oxygen concentration gradient in consideration, but proposed that it was actually the asymmetric interfacial tension gradient, which resulted from the oxygen concentration gradient, that induced a slip velocity at the nanorod–water surface interface (Figure 4a). In consideration of this model, the direction of motion implies that the Au surface is hydrophobic under the conditions of the experiment. The force derived from the interfacial tension gradient is assumed to be continuously re-established as the nanorod moves, which is fundamentally different from the mechanisms of movement of macroscale objects propelled by the same catalytic reaction.

The latest mechanism suggested by the same group was based on self-electrophoresis (Figure 4b), a mechanism often used to describe the migration of particles in a self-generated electric field.[20,36] Lammert et al.[37] considered a biological cell that uses active transport to pump ions into the cell at one end and out at the other. Such a cell would be capable of maintaining a dynamic electric field tangential to the cell surface where ions close to the surface of the cell, in its double layer, would migrate in response to the electric field. That ion migration would cause fluid flow in the interfacial region and a corresponding slip velocity, which ultimately is responsible for the motility of the self-electrophoretic object. The same idea applies to conducting metal nanorods, which are capable of generating their own ion gradients as a result of one end of the particle catalyzing a reduction reaction and the other an oxidation reaction. The details of the electrokinetic mechanism for a Au–Pt nanorod, where the redox disproportionation of the peroxide fuel occurs asymmetrically at the two different metal surfaces, are illustrated in Figure 4b.

Over the past year, there have been a few reports that counter earlier suggested mechanisms for the locomotion of bimetallic nanorods, where the related asymmetry of the catalytic rod surface had been taken as a necessary condition of self-propulsion. We have previously observed that the hydrodynamic behavior of monocomponent catalytic metal nanorods in a solution of H_2O_2 is very similar to the bimetallic ones. Kovtyukhova[38] presented a study on monocomponent rods, concluding that the surface chemical asymmetry is unlikely to be a governing factor in the self-propulsion. The new model, which is based on gravitational forces and considers rod motion in 3D space, provides a reasonable explanation for some motional behavior of the nanorod motors (Figure 4c and d). The oxygen bubble departure from the rod surface causes the momentum exchange between the ''tilted'' rod and water flux, resulting in directional motion of the rod (Figure 4c). Kovtyukhova[38] suggests that the parallel orientation of the

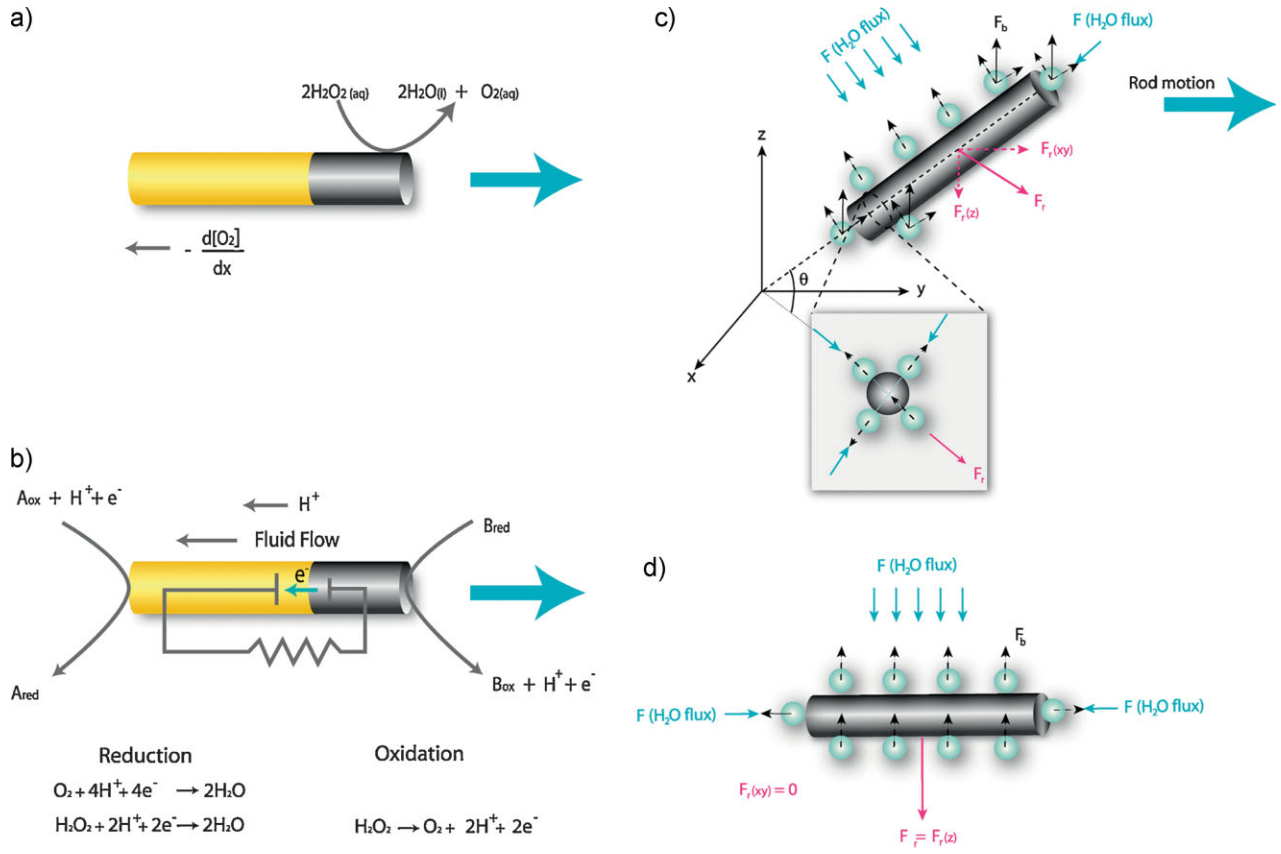

Figure 4. Models of nanorod locomotion. a) Schematic of an asymmetric Au—Pt nanorod driven by the catalytic decomposition of H_2O_2 as a result of an interfacial tension gradient. [14] b) A bimetallic nanorod acting as a redox active particle capable of generating its own dynamic electric field and the corresponding slip-velocity inducing nanorod locomotion. [20] For charge balance to be met the protons must migrate from the Pt end (anode) towards the Au end (cathode) primarily through the electrical double layer at the metal–solution interface. Since the ions in the double layer migrate with respect to the particle surface in response to the self-generated electric field, the particle moves with respect to the fluid. c) Schematic representation of forces acting on a nanorod (F_r) catalyzing oxygen formation in aqueous H_2O_2 solution. The long axis of the nanorod makes an angle θ with the *xy*-plane. d) The long axis of the rod is parallel to the substrate. F_b is the buoyancy force exerted on O_2 bubbles, which is resolved into two components normal and parallel to the rod surface. $F(H_2O)$ is the push by water flux caused by the bubbles' departure. [38]

rod with respect to the substrate is an unfavorable geometry for propulsion, as the bubbles departing from the walls do not generate driving force along the long axis of the rod (Figure 4d).

It was also recently shown that for rotational nanomotors designed in the Mirkin group[39] the electrofluidic mechanism was not a significant contribution to the rotation. Furthermore, rotary Si/Pt nanorods have also been shown to be active in a dilute H_2O_2 solution. The Si/Pt nanorods, an insulator/metal structure, are different from coaxial bimetallic nanomotors.[40] Therefore, there is no electrochemical pathway able to induce electrokinetics in Si/Pt nanorods when exposed to H_2O_2.

8. Stochastic Processes of Mobility Modes of Self-Propelled Nano-objects

An interesting aspect of nanorod locomotion not yet discussed is the variability in motility modes experienced by the self-propelled nano-objects. In any given sample any nanorod could undergo straight autonomous motion, rotate, or orbit at any time. For the most part, rotation has been attributed to an in-built asymmetry[40,41] or imperfections in the preparation method leading to non-uniform catalytic nanorods. In order to explain the observation that one nanorod is actually able to switch from one motility mode into another in a stochastic way, one has to consider the effect of the immediate environment, that is, the substrate, on the motility modes exhibited by the nanorods. Recent hydrodynamic studies on swimming microorganisms in the vicinity of surfaces have indicated that there are strong interactions between swimming cells and solid surfaces that ultimately lead to the reorientation of the mobile species in the direction parallel to the surface.[42] The mobility of *E. coli* is approximated by a force dipole, where the propulsive force that is opposed by the viscous drag on both the cell body and flagella is provided by the flagellar motion. The superposition of the flow induced from a force dipole and any image flow field located on the other side of the surface describes the total flow field induced by the cell. Depending on the interaction between the two flows, a preferential orientation parallel to the surface can occur, as is the case in *E. coli*, but for cells, such as certain algal strains, which are pushed by their flagella motion rather than pulled, the hydrodynamic interactions are such that the cell is reoriented in the perpendicular direction with respect to the substrate, crashing into walls and undergoing rotational motion.

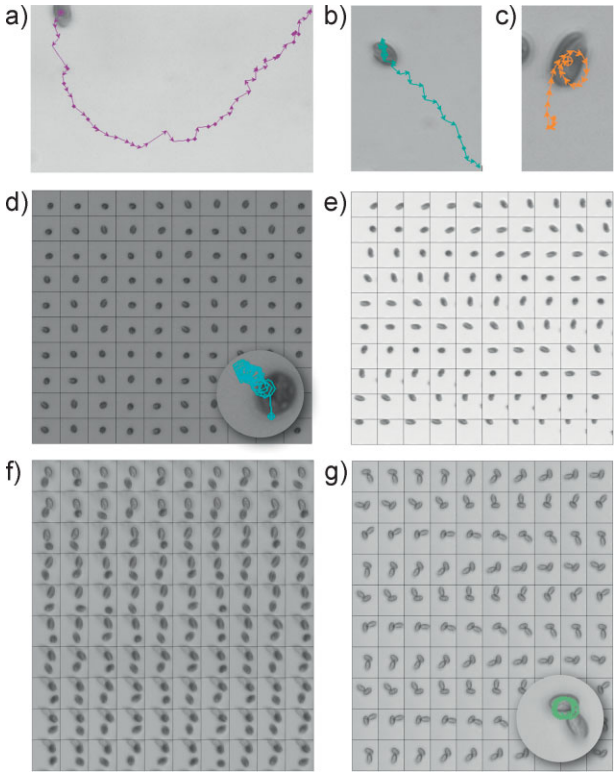

Figure 5. Characteristic motility modes of *Rhodomonas* CS24. Zigzag propulsion tends to be the fastest (a and b), while the addition of rotational components such as in tumbling (c) and revolving/orbiting (d and e) slows the algae down. Pairs of flagellate organisms also display cooperative (g) and non-cooperative (f) induced motion/interactions.

The need for a very general explanation for all the motility behaviors of nanoscale objects, biological and synthetic, is evident by comparing the similarities between the motility behaviors of metal nanorods and a flagellar algae *Rhodomonas* CS24.[43] Their size and diffusion coefficients are almost analogous to those of nanorods. Even though the source of their power used in their mobility, the flagellum, is different than in the chemically driven metal-nanorod systems, they also do exhibit a number of different motility modes (Figure 5). The random change between those mobility styles by one alga is similar to the behavior observed for bimetallic nanorods. These observations are a clear indication that in addition to the different sources of power generation required for the propulsion, the local environmental factors within microdomains of the immediate fluid surroundings and the glass substrate cannot be discounted when considering the mechanisms of locomotion of nanoswimmers.

9. But Why Did It Take So Long?

Over the last 20 years or so we might have been too preoccupied with shorter-term goals that focused attention on trying to understand how to use nanochemistry to gain control over the size, shape, surface, defects, and self-assembly of a ''periodic table of nanomaterials'' and how to utilize these nanomaterials in application areas from nanoelectronics to nanomedicine rather than spend time on more adventurous longer-term objectives like generating, controlling, and utilizing the motion of nanoscale materials to create purposeful nanomachines using nanochemistry. While the nanotechnological enticements enabled by futuristic nanomotors and nanomachines are less certain than the electronic and medical applications of nanomaterials, the challenges of understanding locomotion of nanoscale objects powered by chemical reactions are profound and clearly at the leading edge of nanoscience. Nevertheless, with hindsight it was surprising to discover that the dynamics of Au–Pt and Au–Ni nanorods in aqueous H_2O_2 were so distinctive to that expected for nanorod Brownian motion. What is more surprising is that it took so long to discover!

10. Conclusions

Following these breakthrough experiments on chemically powered nanorod motion the hard work began with a flurry of exciting reports mainly aimed at understanding the physicochemical principles underpinning nanorod propulsion, how to control nanorod speed and direction, and probing effects of viscosity, concentration of fuel, temperature, pH, ionic strength, co-solvents, and fuel gradients on the movement of nanorods. Today the main candidates for the mechanism of nanorod propulsion mentioned earlier are still hotly contended and from an assessment of available reports it seems likely that all of the proposed driving forces contribute to the observed motion to varying extents under different conditions.

At this early point in the development of the field of chemically powered locomotion of nanoscale objects it is worth asking, what's next? Some challenges are listed below:

- ◇ One pivotal step must be to move to the true nanoscale where all dimensions of the nanomotors are in the nanometer range. For example, this could be achieved with Pt-tipped CdSe nanorods or Pt–SiO_2 Janus nanospheres and using nanometer-scale spatial resolution optical methods for monitoring the nanorod motion.
- ◇ Another key requirement for progress is to be able to optically track nanorod motion in all three spatial dimensions rather than two dimensions as employed so far.
- ◇ There is also a dire need to discover new energy rich fuels beyond H_2O_2 that are able to power the nanomotors, like methanol, formic acid, diazomethane, azides, hydrides, organic peroxides, and so forth.
- ◇ Other chemical sources of motion should be sought such as nanomotor etching, de-alloying, and electroless plating reactions as well as on-board polymerizations.
- ◇ A thorough assessment of how the shape of nano-objects and the perfection of shape affect motion is also a high priority.
- ◇ The important role of spatial and surface confinement of nanorods, as found in the channels and chambers of microfluidic chips or at liquid–liquid interfaces, on nanorod dynamics also needs to be explored.

The current interest in designing nano-/micrometer-scale artificial systems that are capable of mimicking biologically

small NANO MICRO

derived self-propellers is tremendous and has transcended into a number of different fields. Inspired by the natural design of bacterial flagella, a top-down approach has recently been employed for the fabrication of artificial bacterial flagella composed of a helical tail and a soft magnetic head whose swimming abilities in 3D have been demonstrated in the presence of weak applied magnetic fields.[44]

The second phase of research in this field should focus on finding these tiny motors some work to do. One of the first important proof-of-concept tasks was recently demonstrated, where autonomously moving Au–Pt nanomotors were able to transport a prototypical cargo.[45,46] The transport of a chemical or biochemical payload from a storage zone to a target site with controlled release of the load might require further functionalization of bar-coded nanorods. The recently demonstrated, magnetically induced bending of a hollow elastic polyelectrolyte hinge that was incorporated into the nanorod heterostructure might provide a possible mechanism for controlled release.[47] If this latter task for nanomotors could be accomplished in a predetermined and reproducible manner then we will be one step closer to futuristic intravascular nanosubmarines delivering payloads to target sites of disease in the human body, and looking further beyond, why not nanomotor-controlled medical procedures within cells?

Acknowledgements

G.A.O. is the Government of Canada Research Chair. He is deeply indebted to the Natural Sciences and Engineering Research Council (NSERC) of Canada for financial support for this work. T.M. thanks NSERC for the graduate scholarship in support of her research. The authors wish to thank Dr. Krystyna E. Wilk and Prof. Paul M. G. Curmi for Rhodomonas CS24 samples.

[1] E. R. Kay, D. A. Leigh, F. Zerbetto, *Angew. Chem. Int. Ed.* **2007**, *46*, 72.
[2] J. Wang, *ACS Nano* **2009**, *3*, 4.
[3] A. Sen, M. Ibele, Y. Hong, D. Velegol, *Faraday Discuss.* **2009**, *143*, 15.
[4] G. A. Ozin, I. Manners, S. B. Fournier, A. Arsenault, *Adv. Mater.* **2005**, *17*, 3011.
[5] B. Yurke, A. J. Turberfield, A. P. Mills, Jr, F. C. Simmel, J. L. Neumann, *Nature* **2000**, *406*, 605.
[6] J. J. Schmidt, C. D. Montemagno, *Annu. Rev. Mater. Res.* **2004**, *34*, 315.
[7] K. Kinosita, R. Yasuda, H. Noji, K. Adachi, *Philos. Trans. R. Soc. London, Ser. B* **2000**, *355*, 473.
[8] K. Namba, F. Vonderviszt, *Q. Rev. Biophys.* **1997**, *30*, 1.
[9] A. Upadhyaya, A. van Oudenaarden, *Curr. Biol.* **2003**, *13*, R-734.
[10] L. A. Cameron, P. A. Giardini, F. S. Soo, J. A. Theriot, *Nat. Rev. Mol. Cell. Biol.* **2000**, *1*, 110.
[11] L. A. Cameron, M. J. Footer, A. van Oudenaarden, J. A. Theriot, *Proc. Natl. Acad. Sci. USA* **1999**, *96*, 4908.
[12] R. K. Soong, G. D. Bachand, H. P. Neves, A. B. Olkhovets, H. G. Craighead, C. D. Montemagno, *Science* **2000**, *290*, 1555.
[13] D. B. Weibel, P. Garstecki, D. Ryan, W. R. DiLuzio, M. Mayer, J. E. Seto, G. M. Whitesides, *Proc. Natl. Acad. Sci. USA* **2005**, *102*, 11963.
[14] W. F. Paxton, K. C. Kistler, C. C. Olmeda, A. Sen, S. K. St, Angelo, Y. Cao, T. E. Mallouk, P. E. Lammert, V. H. Crespi, *J. Am. Chem. Soc.* **2004**, *126*, 13424.
[15] S. Fournier-Bidoz, A. C. Arsenault, I. Manners, G. A. Ozin, *Chem. Commun.* **2004**, 441.
[16] C. R. Martin, *Science* **1994**, *266*, 1961.
[17] M. Tanase, L. A. Bauer, A. Hultgren, D. M. Silevitch, L. Sun, D. H. Reich, P. C. Searson, G. J. Meyer, *Nano Lett.* **2001**, *1*, 155.
[18] J. C. Love, A. R. Urbach, M. G. Prentiss, G. M. Whitesides, *J. Am. Chem. Soc.* **2006**, *125*, 12696.
[19] T. R. Kline, W. F. Paxton, T. E. Mallouk, A. Sen, *Angew. Chem. Int. Ed.* **2005**, *44*, 744.
[20] W. F. Paxton, A. Sen, T. E. Mallouk, *Chem. Eur. J.* **2005**, *11*, 6462.
[21] A. Einstein, *Ann. Phys. (Leipzig, Ger.)* **1905**, *17*, 549.
[22] H. C. Berg, *Random Walks in Biology*, Princeton University Press, Princeton, New Jersey **1983**.
[23] M. Takeo, *Disperse Systems*, Wiley-VCH, Weinheim, Germany **1999**, pp. 43–60.
[24] S. K. St, Angelo, C. C. Waraksa, T. E. Mallouk, *Adv. Mater.* **2003**, *15*, 400.
[25] L. P. Faucheux, A. J. Libchaber, *Phys. Rev. E* **1994**, *49*, 5158.
[26] A. Najafi, R. Golestanian, *Phys. Rev. E* **2004**, *69*, 062901-1.
[27] E. M. Purcell, *Am. J. Phys.* **1977**, *45*, 3.
[28] P. S. Lovely, F. W. Dahlquist, *J. Theor. Biol.* **1975**, *50*, 477.
[29] R. Laocharoensuk, J. Burdick, J. Wang, *ACS Nano* **2008**, *5*, 1069.
[30] U. K. Demirok, R. Laocharoensuk, K. M. Manesh, J. Wang, *Angew. Chem. Int. Ed.* **2008**, *47*, 9349.
[31] N. S. Zacharia, Z. S. Sadeq, G. A. Ozin, *Chem. Commun*, **2009**, 5856.
[32] R. F. Ismagilov, A. Schwartz, N. Bowden, G. M. Whitesides, *Angew. Chem. Int. Ed.* **2002**, *41*, 652.
[33] A. A. Solovev, Y. Mei, E. Bermúdez Urena, G. Huang, O. G. Schmidt, *Small* **2009**, *5*, 1688.
[34] J. Vicario, R. Eelkema, W. R. Browne, A. Meetsma, R. M. La Crois, B. L. Feringa, *Chem. Commun.* **2005**, 3936.
[35] J. M. Catchmark, S. Subraman, A. Sen, *Small* **2005**, *1*, 202.
[36] Y. Wang, R. M. Hernandez, D. J Bartlett, Jr. J. M. Bingham, T. R. Kline, A. Sen, T. E. Mallouk, *Langmuir* **2006**, *22*, 10451.
[37] P. E. Lammert, J. Prost, R. Bruinsma, *J. Theor. Biol.* **1996**, *178*, 387.
[38] N. I. Kovtyukhova, *J. Phys. Chem. C* **2008**, *112*, 6049.
[39] L. Qin, M. J. Banholzer, X. Xu, L. Huang, C. A. Mirkin, *J. Am. Chem. Soc.* **2007**, *129*, 14870.
[40] Y. He, J. Wu, Y. Zhao, *Nano Lett.* **2007**, *7*, 1369.
[41] J. G. Gibbs, Y.-P. Zhao, *Small* **2009**, *5*, 2304.
[42] A. P. Berke, L. Turner, H. C. Berg, E. Lauga, *Phys. Rev. Lett.* **2008**, *101*, 38102-1.
[43] T. Mirkovic, K. E. Wilk, P. M. G. Curmi, G. D. Scholes, *Photosynth. Res.* **2009**, *100*, 7.
[44] L. Zhang, J. J. Abbott, L. Dong, K. E. Peyer, B. E. Kratochvil, H. Zhang, C. Bergeles, B. J. Nelson, *Nano Lett*, DOI: 10.1021/nl901869j.
[45] S. Sundararajan, P. E. Lammert, A. W. Zudans, V. H. Crespi, A. Sen, *Nano Lett.* **2008**, *5*, 1271.
[46] J. Burdick, R. Laocharoensuk, P. M. Wheat, J. D. Posner, J. Wang, *J. Am. Chem. Soc.* **2008**, *130*, 8164.
[47] T. Mirkovic, A. C. Arsenault, S. Fournier-Bidoz, N. S. Zacharia, G. A. Ozin, *Nat. Nanotechnol.* **2007**, *2*, 565.

Received: July 24, 2009
Published online: November 12, 2009

